

Directionality of acoustic T-phase signals in the South Fiji Basin

N. Ross Chapman (1) and Ralph Marrett (2)

(1) School of Earth and Ocean Sciences, University of Victoria, BC, Canada
 (2) Defence Technology Agency, Auckland Naval Base, Auckland, New Zealand

ABSTRACT

Acoustic transients radiated from undersea earthquakes were recorded in an experiment carried out using a towed horizontal line array operating in the South Fiji Basin. The transient signals consisted of P-, S- and T-phases, with strong spectral content in each phase to frequencies as high as 70 Hz. The directionality of the T-phase signal was determined to high spatial resolution by processing the array hydrophone data with a cross spectral beamformer. The T-phase signal was highly directional, and the directivity pattern was different for earthquake events at different sites. For deep earthquakes originating in the fore-arc trench at the northern boundary of the basin, the strongest T-phase components arrived from different directions much farther south of the source, in a region where a number of seamounts and ridges rose within the sound channel. For events originating along the subduction zone arc, the T-phases radiated from slope sites along the ridge to the north. A simple model based on ray path travel times for elastic wave travel in the earth and acoustic wave propagation in the water suggests that the components of the T-phase signal were radiated into the water by downslope propagation from the seamounts and ridges.

INTRODUCTION

Seismic transients from undersea earthquakes have been observed in the ocean over many years (Tolstoy and Ewing 1950; Shurbet and Ewing 1957). The earthquake signal observed in the ocean usually consists of three components, the primary (P), secondary (S) and tertiary (T) phases. The first two components are propagated as elastic waves in the earth and are converted to compressional waves in the water near the receiver, while the T-phase is an acoustic signal that travels in the deep ocean SOFAR (SOund Fixing And Ranging) sound channel (Figure 1). The very low attenuation of signals propagating in the SOFAR channel supports extremely efficient transmission of T-phase energy to very long ranges. Consequently, T-phases provide excellent detection and lo-

calization capability for earthquake events. In recognition of these capabilities, hydroacoustic stations for T-phase detection play a prominent role in the International Monitoring System (IMS) mandated by the Comprehensive Test Ban Treaty Organization (Okal 2001).

Interest in using T-phases to study the details of fault rupture in large earthquakes has also increased since the Sumatra event in December 2004 (de Groot-Hedlin 2005). This application depends on knowing the direction of the T-phase signal, as well as the magnitude. The IMS hydroacoustic stations are designed as triplets of receivers, in order to resolve signal directionality.

Due to the large impedance contrast between the oceanic crust and the water, seismic energy from an earthquake is injected into the water at very high grazing angles. The most widely accepted explanations to describe the generation of oceanic T-phases are: downslope conversion of high-angle bottom interacting energy to shallow-angle SOFAR propagation paths at locations relatively close to the earthquake source (Johnson et al. 1963); or scattering of the seismic energy into the sound channel (Johnson et al. 1968). The scattering mechanism was proposed for T-phase signals that were generated in deep ocean abyssal plains; the higher frequency content and gradual onset of the abyssal T-phase signal was consistent with the scattering hypothesis. By comparison, the slope T-phases are generally lower energy signals with sudden onsets. This behaviour has been observed at Hawaiian hydrophone stations for earthquakes in the North Pacific off Alaska and Japan (Johnson et al. 1963; Walker et al. 1992), and at Polynesian stations for Hawaiian events (Tallandier and Okal 1998). More recent mechanisms proposed by Park et al. (2001) and DeGroot-Hedlin and Orcutt (1999; 2001) have combined the two hypotheses to describe the conversion in terms of scattering along shallow sloping bathymetric features in the vicinity of the epicentre.

Initially, models of T-phase generation focussed on conversion of seismic to acoustic energy near the earthquake location. However, conversion can also take place at more dis-

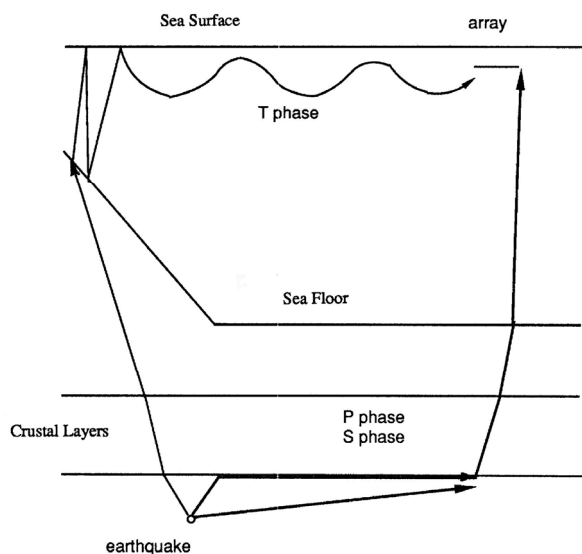


Figure 1. Schematic diagram showing the P and S phase propagation to the array, and to the T-phase generation site on the sloping sea floor. The T-phase propagates via the shallow angle path in the ocean SOFAR channel.

tant sites where the coupling with the SOFAR sound channel is favourable. An example of this behaviour was reported previously in an analysis of seismic transients from a group of three small-magnitude earthquakes that occurred in the New Hebrides Trench at the north-western boundary of the South Fiji Basin (Figure 2) (Chapman and Marrett, 2006). The data used in the analysis were obtained in an experiment using a towed line hydrophone array to study ambient ocean noise processes in the South Fiji Basin. Background noise levels in the basin were expected to be extremely low, about 55–60 dB re 1 μ Pa, due to the very low shipping density and the acoustic isolation of the basin from the rest of the south Pacific by a series of ridges. Consequently, the experiment was able to study noise processes due to winds, marine mammals and small earthquakes that are normally masked by background shipping noise in other parts of the world oceans (Marrett and Chapman, 1993). Seismic events formed a significant contribution to the ambient noise field.

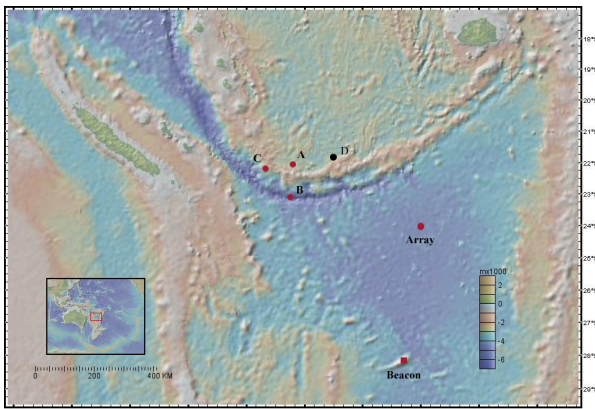


Figure 2. Bathymetry map showing the locations of the array and the earthquakes. The T-phase directionality of events A, B and C was reported in a previous paper.

The line array provided the means to study the directionality of the noise sources that were observed in the experiment to very high spatial resolution. Analysis of the T-phase signals from the group of deep subsea earthquakes revealed the surprising result that the signals were transmitted to the array from sites farther south in the basin, and not only from the epicentre directions. A similar pattern of directionality was resolved in the beamformed T-phase arrival data for each event. In fact, since each event was observed on a different array heading, the true directionality of the T-phase signals was determined in the previous analysis by combining the information of all three events to resolve the left-right ambiguity of the line array (Chapman and Marrett, 2006). Figure 3 shows the directionality versus time obtained for one of the events (event C). The first part of the signal arrives from the direction of the earthquake; however, the signal is generated by scattering from the P and S phases near the array. The subsequent (and stronger) signal components are generated from distant sites along bearings of 260° (beginning at about 240 s), 272° (beginning at about 350 s) and 265° (beginning at about 475 s). Our analysis indicated that the main components of the T-phase signal were radiated from seamounts and ridge sites south of the earthquake location. Only a small fraction of the signal was received from the epicentre direction, starting from about 380 s in the figure. This time corresponded to the travel time to the array from the earthquake location in the water.

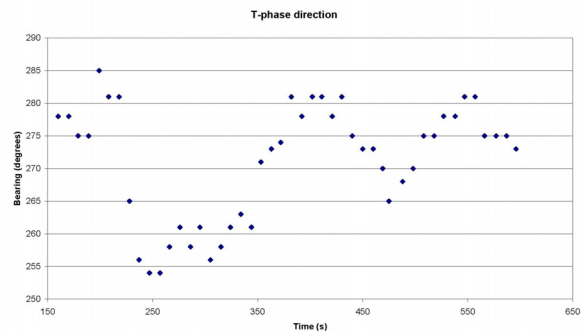


Figure 3. T-phase directionality for one of the deep trench events. The bearing to the epicentre is 284°.

This paper presents a new analysis of the directionality of T-phase signals from a larger undersea earthquake observed in the same experiment. The new event was located east of the other events on the subduction zone arc. The paper is organized as follows. The ambient noise survey experiment with the towed line array is described briefly in the next section. The array data for the new event were processed to obtain the T-phase directionality, and the directionality is interpreted in terms of T-phase generation at sites along the subduction zone arc. The directionality obtained for this event is remarkably different from that observed for the other events in the previous analysis (Chapman and Marrett, 2006). Although the directionality pattern is different, a similar feature is that the T-phase signals are radiated from sites at significant distances from the earthquake location. The paper concludes with a discussion of possible reasons to account for the observed differences.

AMBIENT NOISE SURVEY

The ambient noise data were obtained in an experiment carried out in the South Fiji Basin during July 1982, using a horizontal line array. The array was towed by the New Zealand research ship HMNZS TUI for a period of 12 days in the vicinity of a site at 24° S 176° 10' E (Figure 2). The array consisted of 32 hydrophones spaced equally apart at 9.6 m over an aperture of about 300 m. The towing depth was nominally 400 m, within the SOFAR sound channel, and the ship speed was 2–3 knots. Array straightness and towing depth were monitored by four depth sensors along the aperture, and two heading sensors, one at the head and the other at the tail. Array headings were determined by monitoring the bearing of a signal from a 224-Hz beacon sound source that was deployed at a seamount about 400 km to the south. This signal, together with the array compass data, provided accurate information for determining the array heading to within a degree. In addition to the acoustic data, sound speed profiles were measured at the site throughout the experiment.

The directionality of the noise field was obtained by beamforming the array hydrophone data. The hydrophone data were digitized at a rate of 1024 samples/s and recorded as the primary data at sea. Subsequently, the data were processed with a cross spectral beamformer that used a discrete Fourier transform to carry out the beamforming on the cross spectral averaged fields. The beam spectra (and single channel spectra) were estimated in 1 Hz bins over the band 0–255 Hz, and averaged over periods of ten seconds. The directionality was determined in 63 beams from forward to rear endfire.

The frequency of seismic events was about 2–3 per hour during the experiment. The great majority were either aftershocks or T-phase signals from relatively small earthquakes (magnitude less than 4.0). In this paper we focus on a large earthquake (event D) located east of the smaller magnitude events in the New Hebrides Trench that were analysed previ-

ously. The location, time and focal depth of this earthquake are listed in Table 1, and the source location is shown in the map in Figure 2. The focal depth is much shallower than those of the other three events. The array heading and the range, bearing and P phase travel time for event D are listed in Table 2.

Table 1. Earthquake source information for event D.

Epicentre Location	Time (Z)	Focal Depth	M _b
21.72° S 173.16° E	07/17/ 22:02:05	13 km	5.5

Table 2. Receiving geometry of event D.

Array Heading	Bearing to Epicentre	Range to Epicentre	Travel time
300°	306°	360 km	49 s

EXPERIMENTAL DATA

Single hydrophone

The spectrum of the seismic transient recorded at a single array hydrophone is plotted versus time in the lower panel of Figure 4, where the intensity is indicated by the colour scale in dB relative to the magnitude of the maximum intensity. The signal is limited at low frequencies (< 8 Hz) by flow noise at the towed array; however, there is spectral information in the seismic transient over the band from 10 Hz to at least 70 Hz. The prominent noise feature that appears at all times at higher frequencies between 150–200 Hz is due to marine animals (Marrett and Chapman, 1993).

The time history of this event is different from that of all the other three events reported previously (Chapman and Marrett, 2006). The first arrival consists of only a single phase that lasts about 60 s, compared to the two phase arrivals that were observed in the other events. The T-phase begins about 90 s after the P-phase arrival, and persists for a period of about 11 minutes. However, the array signal was saturated after about 110 s into the event, and the analysis reported here is restricted to the portion of data before saturation. The travel time from the earthquake source to the array is about 49 s for the first phase.

Array directionality data

The time history for the directionality of the seismic transient is shown in array beam space in the upper panel of Figure 4. The data were filtered in the frequency band from 14–16 Hz and processed in beams. The vertical traces for each beam display the beam intensities in the colour scale, from forward to rear endfire (bottom to top in the figure). Each horizontal slice is an average of 10 s of data.

It should be noted here that Figure 4 is designed for convenient presentation of the directionality data; the upper intensity limit is cut off at ~ 90 dB for the display. Although the 3-dB beam width for a signal at 15 Hz is large (~ 17°), the T-phase bearings could be resolved to a much higher accuracy from these data because the signal strength was high over a broad frequency band. The beam signal-to-noise ratio was in excess of 40 dB at 15 Hz, and up to 20 dB at 60 Hz. The directions were determined in practice from frequency-azimuth plots for each 10-s period, using data over the full T-phase band up to 60 Hz. The bearings can be inferred from the display in Figure 4 by interpolating the central peak of the symmetric beams.

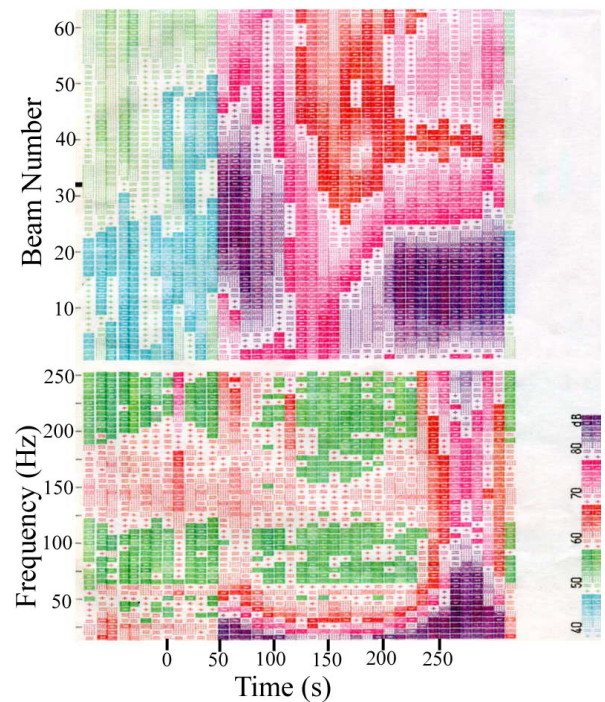


Figure 4. The lower panel shows the time history of the spectrum of the seismic transient from a single hydrophone plotted over the band 15–250 Hz. The upper panel shows the array beam directions of the same signal. The time origin is the event time.

The first phase is received 49 s after the onset of the event in the beams near broadside, which receive energy that propagates at high angles in the water. This is expected on the basis of the model shown in Figure 1 for the propagation of the P or S phases. The energy travels primarily in the earth at speeds characteristic of P and S waves, and is refracted into the water near the array at steep grazing angles due to the large contrast in sound speeds between the ocean sub-bottom material and the water. Assuming that the energy from the seismic wave in the earth is refracted from the sub-bottom material at the critical angle, a crude estimate of the elastic wave speed can be determined by relating the observed beam angle, ψ , to the vertical, ϕ , and azimuthal, θ (measured relative to the array axis), propagation angles. The relationship for the beam angle derived from spherical geometry is:

$$\cos \psi = \cos \theta \cos \phi \quad , \quad 1$$

and the vertical propagation angle is related to the wave speed in the sub-bottom by

$$\cos \phi = \frac{c_w}{c_b} \quad , \quad 2$$

where c_w and c_b are the water and seismic wave sound speeds, respectively. For this event the beam angle is $78^\circ \pm 2^\circ$ and the azimuthal angle to the epicentre is about 5° , so that the sound speed is about 7.2 ± 1 km/s. This value is consistent with expected result for P waves, and is close to the value estimated from the travel time to the event.

T-phase directionality

The T-phase signal is initially observed in a beam near forward endfire about 90 s following the P-phase arrival. The signal subsequently shifts to beams closer to broadside over the next 60 s, and then locks in on a beam about 37° off

broadside. Unfortunately, the T-phase signal from this event saturated the receiving system about 50 s later, and there was no attempt to recover any directional information after that time. However, the pattern of the T-phase direction in the initial portion of the signal was significantly different from that observed for the other three events reported previously.

The true directionality cannot be obtained uniquely from a single event using a line array, so the ambiguous bearings are also listed (in plain type) in Table 3. However, we can use travel time arguments based on the simple propagation model described previously to rule out the bearings to the south of the array (between 240°–260°). The propagation model in Equation 3 assumes that the seismic energy travels as elastic waves in the earth from the earthquake source to the seamounts, and then propagates to the array as water borne acoustic energy in the SOFAR channel at a speed of 1.49 km/s:

$$\tau = \frac{R_b}{c_b} + \frac{R_w}{c_w} \quad 3$$

Here, τ is the total T-phase travel time, and R_b and R_w are the distances in the earth and water, respectively. An inspection of the multibeam bathymetry data (Figure 2) shows that there are no features along these bearings that could generate T-phases with the observed travel times.

Table 3. Array directionality data and travel times for the T-phase components.

T-phase Component	Signal Direction	Observed travel time	Modelled travel time
I	334°±2°/265°±2°	150 s	153 s
II	343°±2°/246°±2°	175 s	173 s
III	352°±2°/248°±2°	195 s	196 s

The resulting directionality is plotted versus time in Figure 5(a), where the reference time is the onset of the event. The intensity (in dB) is also shown (Fig. 5(b)) with respect to the same time origin. The signal is initially resolved on a bearing of ~335°. About 20 s later it shifts to a bearing of ~342°, before shifting again to ~352° where it remains until the signal saturates, approximately 200 s after the time of the P-phase arrival.

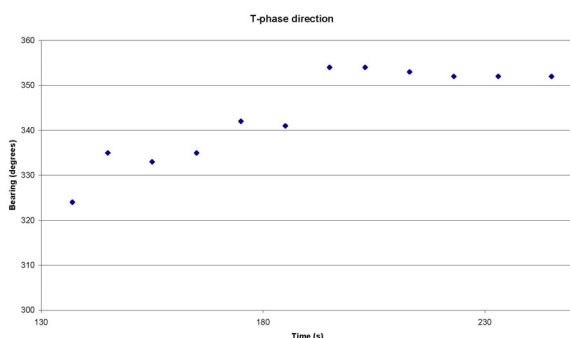


Figure 5(a). Directionality of the T-phase signal from event D versus time. The origin of time is the earthquake event time. The first component arrives on a bearing of 335° at about 145 s; the second component arrives on a bearing of 342° at about 175 s, and the third and strongest component arrives on a bearing of 352° at about 195 s.

These bearings indicate that the T-phase energy is radiated primarily from locations on the ridge slopes east of the epicentre, along the subduction arc directly to the north of the array. This result is quite different from that reported previously for the other group of earthquakes in this region, where the T-phases originated from seamounts and ridge sites to the

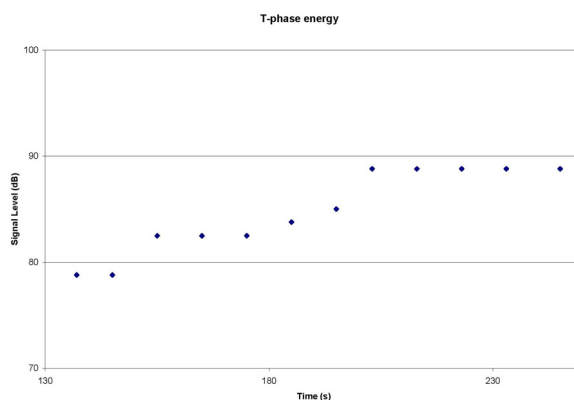


Figure 5(b). Energy of the T-phase signal from event D versus time.

south. However, the behaviour is similar to that reported for the source of T-phase energy in other subduction zone environments, for example in the Indian Ocean, where the T-phases were observed to radiate along the slope between the trench and arc (Graeber and Piserchia, 2004). We propose in the next section a simple model for the T-phase propagation to account for our observations of the directionality.

DISCUSSION

We show in Figure 6 propagation paths for the simple propagation model to account for the observed travel time of the T-phase signals. The propagation paths in the earth are shown in white and the ocean SOFAR paths in black. The bearing to the event is shown by the red line. We do not propose a specific process of seismo-acoustic energy conversion, but the model underlines the importance of downslope conversion in the process. The model assumes that the signals are radiated from specific bathymetric features along the ridge that rise substantially into the water column, to depths as shallow as 2000–2500 m. These features lie along the bearings given in the previous section (Table 3) for the signal direction for each component, as indicated in Figure 5. The measured times and the predicted travel times are also listed in Table 3. The simple propagation model fits the measured travel times very well using P wave propagation speeds in the earth.

Interestingly, the onset of signal saturation coincides with the travel time from the epicentre location to the array at the ocean water sound speed. It is highly probable that a slope T-phase was radiated into the water at the earthquake site; this was also observed for the deeper focus event C. However, it was not possible to determine the directionality of the signal at this time.

The different behaviour observed for this earthquake is likely due to the location and characteristics of the event itself. Compared to the other events that were located very deep in the New Hebrides Trench (focal depths > 33 km), event D was a shallow earthquake that occurred directly beneath the ridge.

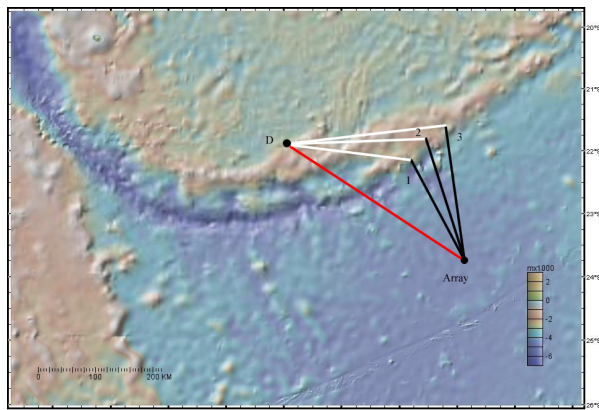


Figure 6. Directions of T-phase components for event D. The signal directions for the T-phase components are distinct from the direction to the earthquake source, and extrapolate to slope features on the ridges to the north. The calculated travel times in Table 3 are based on T-phase generation sites indicated by the intersections of the white and black lines.

It is instructive to discuss another possible interpretation for the observed signal directionality from event D. The alternate explanation is based on the interpretation of the T-phase signals from the December 2004 Sumatra event. The undersea fault rupture for that event extended for several hundred km, propagating at supersonic speeds. The source of both P and T phases extended along the rupture, and in fact, the T-phase directionality was used to map the length of the fault rupture itself. Although it is tempting to apply the same explanation to interpret the T-phase directionality from event D, it is highly unlikely to be the correct interpretation. From Figure 6, the fault rupture would have to propagate a distance of about two hundred km along the ridge to generate the observed directionality. Since the fault rupture length scales roughly by factors of ten with the event magnitude, it is unlikely that the rupture for event D (less than magnitude 6 compared to 9 for the Sumatra event) extended over such a large distance. Furthermore, the observed T-phase travel times are not consistent with the extended fault rupture interpretation.

SUMMARY

The directionality of T-phases from an undersea earthquake originating at the northern margin of the South Fiji Basin was determined to high resolution using a towed horizontal line array. The T-phase direction pattern resolved from this event was strikingly different from that associated with a group of three small magnitude events that occurred at much deeper depths farther west in the New Hebrides Trench. A simple model for the travel times of the T-phase components, based on propagation from the earthquake source to the ridge slopes at elastic wave speeds in the earth followed by propagation from these features to the array in the sound channel was consistent with the measured data. The model assumes that the seismic energy is coupled to the ocean efficiently at the

ridge slopes. The conversion efficiency is likely related to the local sea floor slope and sea bed roughness at the conversion site.

REFERENCES

- Chapman, N.R. and Marrett, R., The directionality of acoustic T-phase signals from small magnitude submarine earthquakes, *J. Acoust. Soc. Amer.*, 119, 3669-3676, 2006.
- de Groot-Hedlin, C.D. and Orcutt, J.A., Synthesis of earthquake generated T-waves, *Geophys. Res. Lett.*, 26, 1227-1230, 1999.
- de Groot-Hedlin, C.D. and Orcutt, J.A., Excitation of T-phases by sea floor scattering, *J. Acoust. Soc. Amer.*, 109, 1944-1954, 2001
- de Groot-Hedlin, C.D., Estimation of the rupture length and velocity of the great Sumatra earthquake of Dec. 26, 2004 using hydroacoustic signals, *Geophys. Res. Lett.*, 32, L11303, doi:10.1029/2005GL022695.
- Graeber, F.M. and Piserchia, P-F., Zones of T-wave excitation in the NE Indian ocean mapped using variations in backazimuth over time obtained from multi-channel correlation of IMS hydrophone triplet data, *Geophys. J. Int.* 158, 239-256, 2004.
- Johnson, R.H., Northrop, J. and Eppley, R., Sources of Pacific T-phases, *J. Geophys Res*, 68, 4251-4260, 1963.
- Johnson, R.H., Norris, R.A. and Dunnebie, F.K., Abyssally generated T phases, in *The Crust and Upper Mantle of the Pacific Area*, L. Knopoff, C.L. Drake and P.J. Hart, editors, Am. Geophys. Union Geophysical Monograph 12, pp 70-78, 1968.
- Marrett, R. and Chapman, N.R., Low frequency noise measurements in an ambient environment dominated by natural sources of sound, in *Natural Physical Sources of Underwater Sound*, B. Kerman, editor, Kluwer Academic publishers, Dordrecht, 1993, pp121-136.
- Okal, E.A., T-phase stations for the international monitoring system of the Comprehensive Nuclear Test Ban Treaty: A global perspective, *Seism. Res. Lett.*, 72(2), 186-195, 2001.
- Park, M., Odom, R.I. and Soukup, D.J., Modal scattering: a key to understanding oceanic T-waves, *Geophys. Res. Lett.*, 28, 3401-3404, 2001.
- Shurbet, D.H. and Ewing, M.W., T-phases at Bermuda and transformation of elastic waves, *Bull. Seism. Soc. Am.*, 47, 251-262, 1957.
- Talandier, J., and Okal, E.A., On the mechanism of conversion of seismic waves to and from T-waves in the vicinity of island shores, *Bull. Seism. Soc. Amer.*, 88, 621-632, 1998.
- Tolstoy, I. and Ewing, M.W., The t-phases of shallow focus earthquakes, *Bull. Seismol. Soc. Am.*, 40, 25-51, 1950.
- Walker, D.A., McCreery, C.S. and Hiyoshi, Y., T-phase spectra, seismic moments and tsunamigenesis, *Bulletin of the Seismological Society of America*, 82, 1275-1305, 1992.